

Synergistic Catalytic Effects of Carbon Nanotube and Nano-Sized TiO₂ on the Hydrogen Sorption of Magnesium Hydride

FAN MEI-QUIANG*[†], SUN LI-XIAN[†] and FEN XU[‡]
*Department of Materials Science and Engineering,
China Jiliang University, Hangzhou-310018, P.R. China
Tel: (86)(571)86835738; E-mail: fanmeiqiang@126.com*

Different TiO₂ such as anatase, rutile and sintered C/anatase were added to magnesium hydride by high-energy ball milling in order to improve the hydrogenation properties of magnesium hydride. The results showed that sintered C/anatase were easily distributed uniform in the MgH₂ matrix and resulted in the good hydrogen sorption of magnesium hydride such as the faster kinetic of hydrogenation and good cycling. Its excellent properties came from the synergistic catalytic effect of TiH formed after de/hydrogenation cycles and nano carbon tubes.

Key Words: Magnesium hydride, Hydrogen storage material, Rutile, Anatase, Synergetic catalytic effect.

INTRODUCTION

The development of H₂ fuel cells for vehicles and mobile applications is very important to reduce greenhouse gas emission and pollution from the burning of fossil fuels. The practical application of fuel cells is decided by many technical challenges such as good hydrogen storage materials. Many work have been developed to design high capacity in moderate conditions, lower cost and safe hydrogen storage materials. Among the different hydrogen storage systems¹⁻⁴, magnesium hydride is regarded as the effective hydrogen storage material as it has a high hydrogen capacity (7.6 wt. %). However, there are still some obstructions such as the low kinetics and the high sorption/desorption temperature to limit its application.

The improved sorption kinetics of magnesium hydride have been achieved *via* the nanocrystalline form obtained by mechanical milling and transition-metal system^{5,6} as milling additives. For example, Wang⁷ reported that TiO₂ had the highest potential as a catalyst for improving the hydrogen sorption properties of metal hydride. TiO₂ (rutile) could provide an effective path for hydrogen penetration of MgH₂-TiO₂ composite systems and dissociation of hydrogen molecules. Croston found that oxide materials based on TiO₂⁸ have been prepared from alkoxide precursors using

[†]Materials and Thermochemistry Laboratory, Dalian Institute of Chemical Physics, Chinese Academy of Sciences, Dalian-116023, P.R. China. Tel: (86)(411)84379213; E-mail: lxsun@dicp.ac.cn

[‡]College of Chemistry and Chemical Engineering, Liaoning Normal University, Dalian-116029, P.R. China.

a sol-gel route and had significantly increased hydrogenation rates of MgH_2 . Jung⁹ thought that the dispersion of TiO_2 in the MgH_2 composite had great effect on the hydrogenation properties of MgH_2 systems. He found that the sample containing 5 mol % rutile had good dispersion in the MgH_2 composite and had higher hydrogen capacity than the sample containing 5 mol % anatase. In spite of many researches carried out on the Mg-TiO_2 system, it was hard to satisfy the capacity requirement of hydrogen storage system. Recently, carbon nanotubes was also a superior additive to improve the hydrogen absorption property of Mg. The MgH_2 -SWNTS composite (single-walled carbon nanotubes)¹⁰ could absorb 6.7 wt % of hydrogen within 100 s at 20 atm H_2 and 573 K. And the metal/alloy catalyst particles in SWNTs could enhance H-absorption of Mg.

Therefore, the composites of MgH_2 and sintered C/ TiO_2 were synthesized by high energy ball milling and their hydrogenation properties were investigated. The aim of this work is to improve the hydrogen storage capacity and hydrogenation kinetics of MgH_2 through synergistic catalytic effect of nano carbon tubes and TiO_2 .

EXPERIMENTAL

The sintered C/ TiO_2 composite was synthesized *via* multi-wall carbon nanotube and TiCl_3 solution as the following reaction in the 1:1 stoichiometric ratio (corresponding weight of multi-wall carbon nanotube and TiCl_3 in the mixture were 0.12 and 1.535 g, respectively). Multi-wall carbon nanotube and TiCl_3 solution were dipped in the dense nitric acid and mixed equally in the 5 h milling. Then ammonia was slowly added in the ceaseless stirring. After filtration, the water solution was removed under the reduced pressure and the black solid obtained was dried at 723 K. The TiO_2 phase and wt % multi-wall carbon nanotube can be confirmed in Fig. 1. The sintered C/ TiO_2 composite has 40 nm size and 12 wt % carbon content from the calculation.

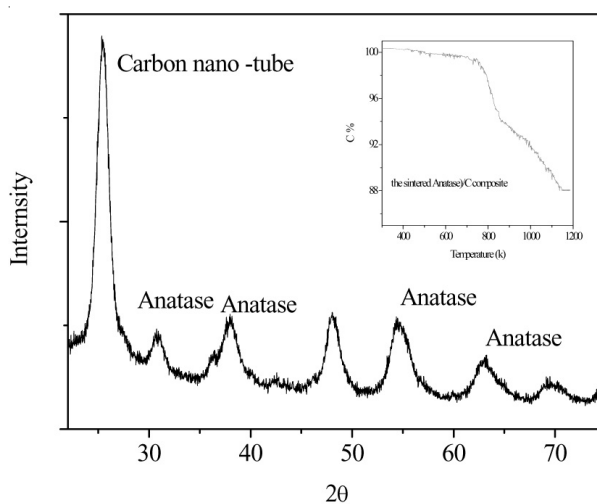


Fig. 1. XRD Patterns of sintered C/anatase

The starting materials for ball milling were MgH₂ powder (98 %, Alfa Aesa) and different TiO₂ (200 nm rutile, 30 nm rutile, 30 nm anatase, sintered C/anatase), shown in Table-1. The molar ratio of MgH₂ and the additive was 95:5. The composites were mixed in an argon-filled glove box to prevent oxidation of the samples and the mixtures were loaded in the 50 mL hardened steel pots with a ball-to powder ratio corresponding to 60:1. The sealed pots were removed from the argon glove box and put on a QM-1SP planetary ball miller. Then milling was performed at 450 r/min for 10 h in Ar atmosphere. After milled, the mixtures were taken out in the argon-filled glove box for the following experiments.

TABLE-1
CHARACTERIZATIONS OF STARTING MATERIALS

	Powder MgH ₂	Rutile	Anatase	Sintered C/anatase
Purity	98	99.5	99.5	99.5
Size	40 nm	20-30 nm	20-30 nm	40-50 nm
Shape	Tetragonal (primitive)	Tetragonal (primitive)	Tetragonal (BBC)	Tetragonal (BBC)

The hydrogenation kinetics of the samples was determined by the conventional Sievert-type P-C-T apparatus. 0.6 g sample was measured and put in steel circular tube and the tube was loaded into a stainless steel reactor in argon box. The hydrogenation experiments were carried out under 10 atm H₂ with the purity of 99.9999 %. The experimental temperature was at the temperature of 473 and 573 K, respectively after initial dehydrogenation in 673 K and 0.001 atm H₂ for 5 h. Powder X-ray diffraction studies were carried out on a DRON-2 diffractometer (crystalline silicon is the internal standard). The dehydrogenation performance of the ball-milling composite was also examined by using diffraction scanning calorimetric (DSC, Setaram DSC141) with high-purity Ar (purity > 99.999 %) as the purge gas at a heating rate of 10 K min⁻¹. Microstructure studies were performed on Joel JEM-20 for TEM images and SAD.

RESULTS AND DISCUSSION

From Fig. 2, it can be found that the decomposition temperatures of the MgH₂ composites have some changes *via* the different additives. About 10 K can be obtained, comparing the additives of sintered C/TiO₂ and carbon nanotube. Fig. 3 shows the hydrogenation kinetics of MgH₂ composites. MgH₂-(30 nm rutile)_{0.05} and MgH₂-(30 nm anatase)_{0.05} have fast hydrogenation kinetics of 5.43 wt % hydrogen and 4.82 wt % hydrogen in 10 min at 573 K, respectively. They can also absorb 4.81 and 4.73 wt % hydrogen in 10 min at 473 K. At the same conditions, the MgH₂-(carbon tube)_{0.05} have 4 wt % at 573 K and 2.5 wt % at 473 K. However, MgH₂-(sintered C/anatase)_{0.05} displays higher hydrogen capacity (5.52 wt % hydrogen in 10 min at 573 K and 4.85 wt % in 10 min at 473 K) and faster absorption kinetics, although the particle size of 40 nm sintered C/anatase is larger than 30 nm rutile.

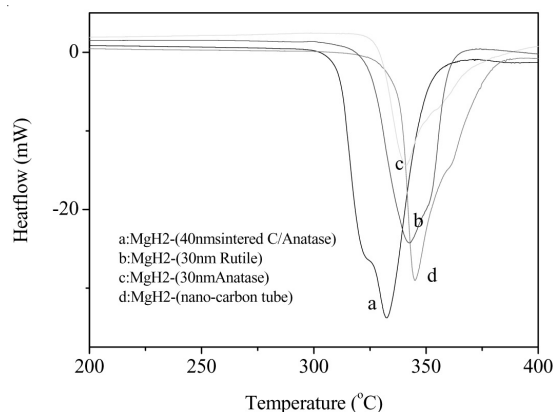


Fig. 2. DSC curves of the MgH_2 composite in the heat rate of 10 K min^{-1} at the Ar atmosphere

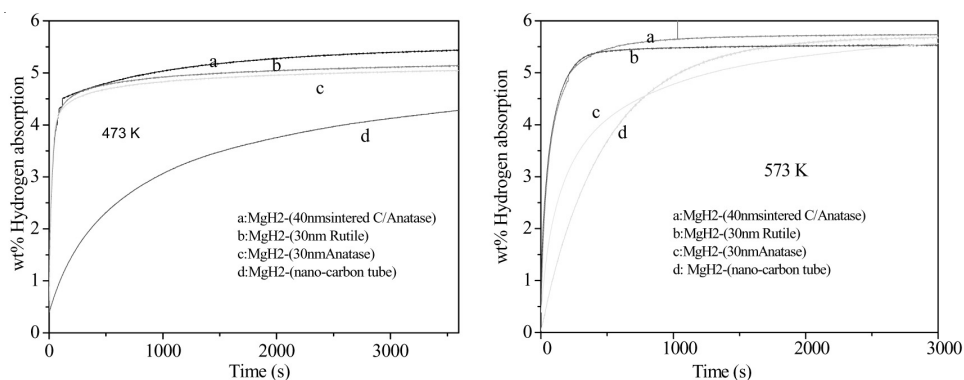


Fig. 3. Hydrogenation kinetics of MgH_2 composites at different temperatures and 10 atm

The improvement is relative to the additive carbon nanotube which favored to the uniform disperse of anatase in Mg matrix in the milling process. Furthermore, the synergetic catalytic effect¹¹ of carbon nanotube and TiO_2 may be occur and responsible for the kinetic enhancement and H-capacity increase, respectively.

Fig. 4 shows the curves of wt % hydrogenation and H_2 pressure at 573 K. It can be found that the mixtures can absorb 0.5 wt % hydrogen at 2.5 atm hydrogen pressure and 3 wt % at 5 atm hydrogen pressure. The wt % hydrogen hydrogenation increases with the higher hydrogen pressure. Therefore, the mixtures can absorb 5.5 wt % hydrogen at 10 atm hydrogen (confirmed in Fig. 4) and 6.4 wt % hydrogen at 20 atm hydrogen. Carefully comparing their wt % hydrogen, the MgH_2 -(30 nm rutile)_{0.05} have a little higher hydrogen capacity than that of MgH_2 -(30 nm anatase)_{0.05}. However, MgH_2 -(sintered C/anatase)_{0.05} has highest hydrogen capacity among the mixtures and the hydrogen capacity was up to 6.6 wt %. The enhancement of the MgH_2 -(sintered C/anatase)_{0.05} come from that it possesses significant advantages: a

large volume fraction and the nanostructure of carbon nano-tube may provide additional diffusion channels for diffusion of hydrogen atoms¹⁰.

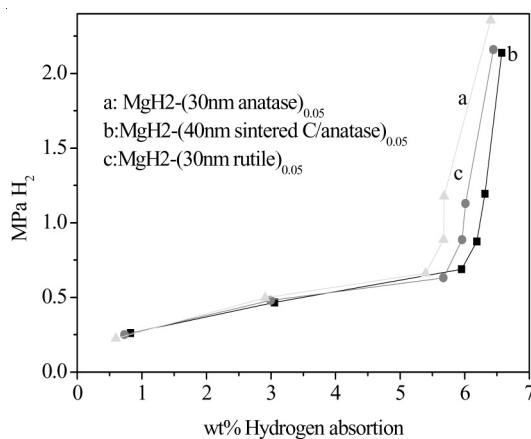


Fig. 4. Hydrogenation isotherm for the MgH₂-composites at 573 K

Fig. 5 shows the cycling of the MgH₂-(30 nm rutile)_{0.05} and MgH₂-(sintered C/anatase)_{0.05} at 573 K. The kinetic of hydrogen hydrogenation of MgH₂-(sintered C/anatase)_{0.05} does not decrease drastically with the cycling number increasing. And the hydrogen capacity has no decrease evidently, only reducing 2.5 % from the first cycling to the tenth cycling, comparing to 3.14 % of MgH₂-(30 nm rutile)_{0.05}. Obviously, the MgH₂-(sintered C/anatase)_{0.05} composites have good stability of high hydrogen capacity.

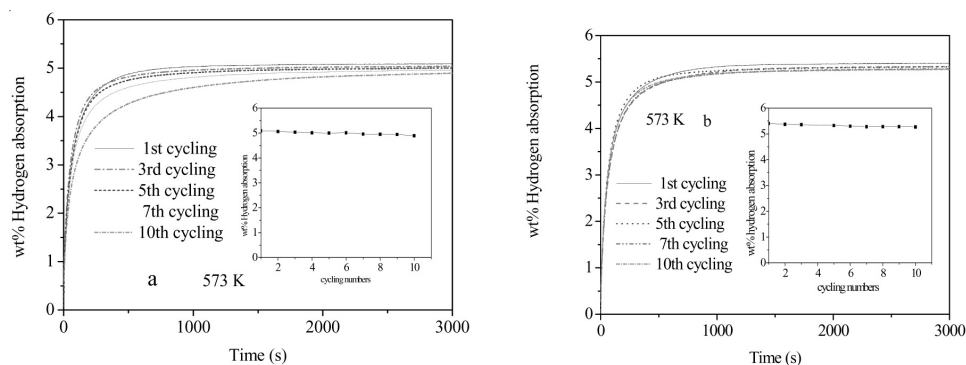


Fig. 5. Hydrogenation kinetics of MgH₂-(30 nm rutile)_{0.05} (a), MgH₂-(sintered C/anatase)_{0.05} (b) in different cycling at 573 K

Fig. 6 shows that the hydrogen capacity of MgH₂-(nm sintered C/anatase)_{0.05} increases from 4.73-5.63 wt % in 10 min at 473 K when the initial hydrogen pressure increases from 10-20 atm. The hydrogen capacity also has the distinct improvement

with the initial pressure increasing in the hydrogenation process in the MgH_2 -(sintered C/anatase) $_{0.05}$ at 473 K. The high hydrogen pressure may facilitate the dissociation of hydrogen molecules on the surface of Mg particles. The increase of hydrogen concentration chemisorbed on the surface of Mg particles will result in an enhanced thermodynamic driving force of hydrogenation.

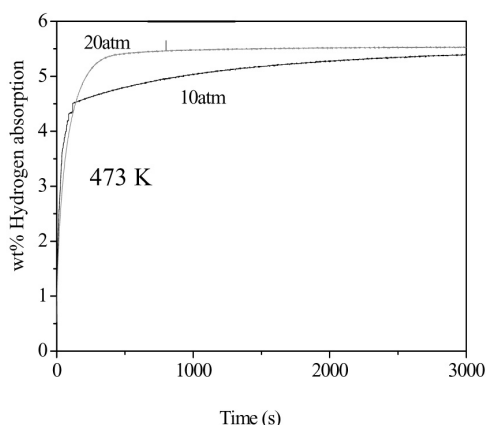


Fig. 6. Hydrogenation kinetics of MgH_2 -(sintered C/anatase) $_{0.05}$ in different hydrogen pressure at 473 K

Fig. 7 shows XRD patterns of the after-cycled MgH_2 - TiO_2 composites. It can be seen that all MgH_2 mixtures show the same characteristic peaks in the XRD patterns, *i.e.*, the dominated peaks of MgH_2 , a few peaks of Mg, MgO and TiH. Characteristic peaks of TiO_2 (rutile or anatase) in the MgH_2 mixtures were not observed. Obviously, the TiO_2 (rutile or anatase) has been deoxidized to TiH after dehydrogenation/hydrogenation cycling. This agrees with the result of the previous report of Jin¹¹. The carbon nanotube may be contributed to the disperse of TiO_2 in the composites. The synergistic catalytic effect with TiH provide a pathway for the form of hydrogen molecule. Fig. 8 shows a representative TEM micrograph and SAD patterns of the cycled MgH_2 -(sintered C/anatase) $_{0.05}$. The sample consists of large MgH_2 particles of 300 nm and small powder of carbon nanotube of 5-15 nm and TiH around 40-50 nm. This morphology shows that the MgH_2 -(sintered C/anatase) $_{0.05}$ nanocomposite may have been formed due to the cold welding and fracture in the milling process. This observation was also found by Wang *et al.*⁷ who thought that MgH_2 and rutile could form nanocomposite. SAD Patterns of MgH_2 -(sintered C/anatase) $_{0.05}$ shows two dark diffraction rings of carbon nano-tube and nano anatase TiH, it also has the diffraction spots of MgH_2 due to the relatively large grain size of MgH_2 .

Conclusion

The different MgH_2 -composites were investigated to enhance the hydrogenation properties of Mg. The results showed that the MgH_2 -(sintered C/anatase) $_{0.05}$ displayed

higher hydrogen properties of 5.52 wt % hydrogen in 10 min at 573 K and 4.85 wt % hydrogen in 10 min at 473 K. The enhancement of hydrogenation kinetics came from the synergistic catalytic effect of carbon nanotube and TiH formed in the sorption/desorption cycling.

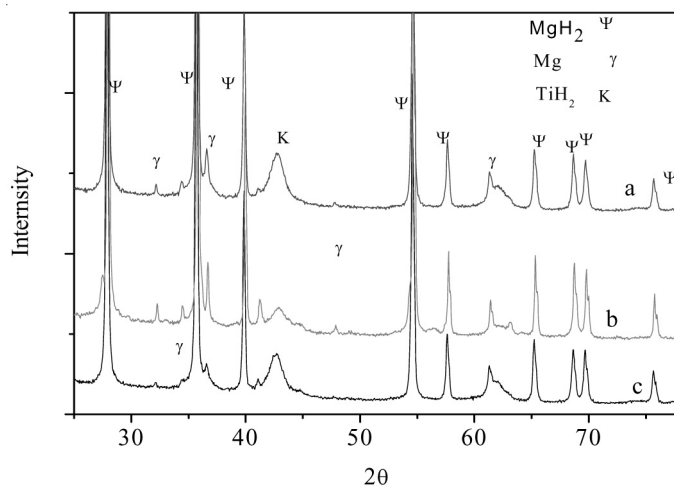


Fig. 7. XRD patterns of the after-cycled; (a) MgH₂-(30 nm anatase)_{0.05}, (b) MgH₂-(30 nm rutile)_{0.05}, (c) MgH₂-(sintered C/anatase)_{0.05}

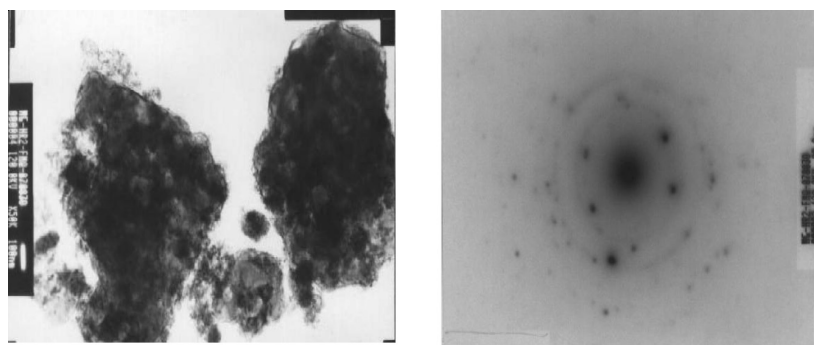


Fig. 8. TEM micrograph and SAD patterns of the cycled MgH₂-(40 nm sintered C/anatase)_{0.05}

ACKNOWLEDGEMENTS

The authors gratefully acknowledged the financial support for this work from the National Natural Science Foundation of China (No. 2083309, 20873148, 50671098 and U0734005), the National High Technology Research and Development Program of China (2007AA05Z115 and 2007AA05Z102), the National Basic Research program (973 program) of China (2010CB631303 and the Zhejiang Basic Research Program of China (Y4090507).

REFERENCES

1. D.P. Broom, *Int. J. Hydrogen Energy*, **32**, 4871 (2007).
2. R. Strobel, J. Garche, P.T. Moseley, L. Jorissen and G. Wolf, *J. Power Sources*, **159**, 781 (2006).
3. M. Yoshino, K. Komiya, Y. Takahashi, Y. Shinzato, H. Yukawa and M. Morinaga, *J. Alloys Compd.*, **404**, 185 (2005).
4. K.M. Thomas, *Catal. Today*, **120**, 389 (2007).
5. N. Hanada, T. Ichikawa, S. Hino and H. Fujii, *J. Alloys Compd.*, **420**, 46 (2006).
6. E. Reguera, *Int. J. Hydrogen Energy*, **34**, 9163 (2009).
7. P. Wang, A.M. Wang, H.F. Zhang, B.Z. Ding and Z.Q. Hu, *J. Alloys Compd.*, **313**, 218 (2000).
8. D.L. Croston, D.M. Grant and G.S. Walker, *J. Alloys Compd.*, **492**, 251 (2010).
9. K.S. Jung, D.H. Kim, E.Y. Lee and K.S. Lee, *Catal. Today*, **120**, 270 (2007).
10. C.Z. WU, P. Wang and X. Yao, *J. Phys. Chem. B*, **109**, 22217 (2005).
11. S.-A. Jin, J.-H. Shim, Y.W. Cho and K.-W. Yi, *J. Power Sources*, **172**, 859 (2007).

(Received: 20 November 2009;

Accepted: 7 May 2010)

AJC-8684

**EUROPEAN WINTER CONFERENCE ON PLASMA
SPECTROCHEMISTRY**

30 JANUARY — 4 FEBRUARY, 2011

ZARAGOZA, SPAIN

Contact:

Secretary: María S. Jiménez

Environmental Sciences Institute (IUCA)

Analytical Spectroscopy and Sensors Group (GEAS)

University of Zaragoza

C/ Pedro Cerbuna 12. F. Ciencias, Ed. D. 1^a Planta

50009 ZARAGOZA-SPAIN

Phone: +34 976 76 22 57, Fax: +34 976 76 12 92

E-mail: winterzar2011@unizar.es